Molecular Biology of the Cell
Vol. 21, 3669–3679, November 1, 2010

An Outer Arm Dynein Conformational Switch Is Required for Metachronal Synchrony of Motile Cilia in Planaria

Panteleimon Rompolas, Ramila S. Patel-King, and Stephen M. King

Department of Molecular, Microbial, and Structural Biology, University of Connecticut Health Center, Farmington, CT 06030-3305

Submitted April 28, 2010; Revised July 21, 2010; Accepted September 7, 2010
Monitoring Editor: Tim Stearns

Motile cilia mediate the flow of mucus and other fluids across the surface of specialized epithelia in metazoans. Efficient clearance of peri-ciliary fluids depends on the precise coordination of ciliary beating to produce metachronal waves. The role of individual dynein motors and the mechanical feedback mechanisms required for this process are not well understood. Here we used the ciliated epithelium of the planarian *Schmidtea mediterranea* to dissect the role of outer arm dynein motors in the metachronal synchrony of motile cilia. We demonstrate that animals that completely lack outer dynein arms display a significant decline in beat frequency and an inability of cilia to coordinate their oscillations and form metachronal waves. Furthermore, lack of a key mechanosensitive regulatory component (LC1) yields a similar phenotype even though outer arms still assemble in the axoneme. The lack of metachrony was not due simply to a decrease in ciliary beat frequency, as reducing this parameter by altering medium viscosity did not affect ciliary coordination. In addition, we did not observe a significant temporal variability in the beat cycle of impaired cilia. We propose that this conformational switch provides a mechanical feedback system within outer arm dynein that is necessary to entrain metachronal synchrony.

INTRODUCTION

Motile cilia located on the surface of epithelial tissues are required for many physiological functions in metazoans. The primary role of these cilia is to mediate the flow of mucus and other extracellular fluids. In humans, ciliated epithelia are present in many tissues including the respiratory tract, the ependyma of the brain, and the fallopian tubes of the female reproductive system. Dysfunctional ciliary movement leads to primary ciliary dyskinesia (PCD; OMIM: 24440) and is responsible for many abnormal conditions such as recurring respiratory infections, infertility, and hydrocephalus (Fliegauf *et al.*, 2007; Ibanez-Tallon *et al.*, 2003; Afzelius, 2004; Ibanez-Tallon *et al.*, 2004; Gu *et al.*, 2005). Furthermore, the epidermis of many invertebrates, including gastropods and turbellarians, consists of a ciliated epithelium and it is thought that the gliding motion of these organisms is achieved through the concerted action of motile cilia upon a secreted mucus layer (Kaiser, 1960; Dorey, 1965; Miller, 1974).

A key characteristic of ciliated epithelia is the coordination of the oscillations of neighboring cilia and the formation of metachronal waves (Gheber and Priel, 1989). In planarians, metachronal waves appear as arrays of cilia in successive phases of their beat cycle and are created when neighboring cilia have a fixed phase difference along the axis of the stroke but beat synchronously perpendicular to the same axis. Metachronal synchrony of beating cilia is important for effective clearance of mucus and transport of other peri-ciliary fluids over the surface of the epithelium. Although, the precise mechanism of wave formation and maintenance is currently unclear, it is thought that hydrodynamic coupling between neighboring cilia is important for metachronal synchrony and that cilia contain systems that provide mechanical feedback to maintain the synchrony. However, the molecular nature of this system(s) and whether cilia actively control the creation and regulation of metachronal waves is unknown.

Ciliary motility is powered and coordinated by the concerted action of inner and outer arm dynein motors, which are multisubunit complexes attached to the outer surface of the peripheral microtubule doublets. The *Chlamydomonas reinhardtii* outer dynein arm particle consists of three distinct heavy chains (HCs), which hydrolyze ATP and mediate the translocation of the motor on microtubules, as well as two different intermediate chains (ICs) and 11 light chains (LCs) that are required for assembly and regulation of the complex (King and Kamiya, 2008). Mutations that compromise the assembly, structural integrity, and function of the outer arm dynein motor result in a significant decrease of beat frequency, reduced swimming velocity, and a characteristic "jerky" swimming pattern (Rutland *et al.*, 1983; Kamiya and Okamoto, 1985; Mitchell and Rosenbaum, 1985). The specific

This article was published online ahead of print in *MBoC in Press* (http://www.molbiolcell.org/cgi/doi/10.1091/mbc.E10–04–0373) on September 15, 2010.

Address correspondence to: Stephen King (king@neuron.uchc.edu).

Abbreviations used: CBF, ciliary beat frequency; DIC, differential interference contrast; HC, heavy chain; IC, intermediate chain; IDA, inner dynein arm; IFT, intraflagellar transport; LC, light chain; ODA, outer dynein arm; PCD, primary ciliary dyskinesia; RNAi, RNA interference; SEM, scanning electron microscopy; TEM, transmission electron microscopy.

role of outer arm dynein in metachronal synchrony of beating cilia has not been explored.

Previous studies have indicated the presence of various regulatory cues that act on dynein motors and control their function and enzymatic activity through phosphorylation, Ca^{2+}, cAMP and redox poise (Hyams and Borisy, 1978; Bessen *et al.*, 1980; Hasegawa *et al.*, 1987; Habermacher and Sale, 1997; King and Dutcher, 1997; Wakabayashi and King, 2006). In addition, two copies of a highly conserved light chain (LC1) associate directly with the motor domain of the *Chlamydomonas* outer arm γ HC (Pfister *et al.*, 1982; Benashski *et al.*, 1999). Down-regulation of LC1 expression by RNAi in *Trypanosoma* leads to motility defects (Baron *et al.*, 2007). However, this phenotype may be the result of pleiotropic effects as the LC1 knockdown strains also exhibited impaired outer arm dynein assembly and mis-orientation of the central pair complex. Expression of dominant-negative LC1 mutant proteins in wild-type *Chlamydomonas* showed no assembly defects but significant alterations in waveform. Mechanical activation of mutant flagella revealed that axonemes contain two mechanosensory systems: one associated with the inner arms and radial spokes and a second that acts on the outer arms (Hayashibe *et al.*, 1997). Together these observations suggest that LC1 acts in a conformational switch to regulate outer arm motor activity in response to alterations in flagellar curvature (Patel-King and King, 2009). To date no LC1-null mutants have been identified in any organism.

To assess the role of outer arm dynein in metachronal synchrony of beating cilia and to determine whether LC1-mediated conformational switching is involved in this process, we used *Schmidtea mediterranea*, a species of planarian flatworm, which possesses a well-defined ciliated epithelium, as a model system to study loss-of-function effects (Newmark *et al.*, 2003; Rompolas *et al.*, 2009). We demonstrate that impairment of outer arm dynein assembly caused a significant drop in ciliary beat frequency (CBF) and abolished the ability of beating cilia to form metachronal waves. Furthermore, we found that this phenotype is due to the lack of an outer arm-associated conformational switch and is not caused merely by a reduction in CBF or a significant variability in the duration of the beat cycle of impaired cilia. Our data suggest that outer arm dynein actively participates in the formation and maintenance of metachronal waves in ciliated epithelia and that LC1 is an essential regulator of this process.

MATERIALS AND METHODS

Planarian Strain and Culture Conditions

The hermaphroditic sexual strain (Zayas *et al.*, 2005) of *S. mediterranea* used in this study was a generous gift of B. R. Graveley (University of Connecticut Health Center) and originated from the laboratory of A. Sánchez Alvarado (University of Utah). Planarians were maintained in a 1× solution of Montjuïc salts (1.6 mM NaCl, 1.0 mM $CaCl_2$, 1.0 mM $MgSO_4$, 0.1 mM $MgCl_2$, 0.1 mM KCl, 1.2 mM $NaHCO_3$; Cebria and Newmark, 2005), in a dark incubator at 21°C. Animals were fed twice a week with homogenized calf liver, and the colony was expanded by repeated cycles of cutting larger planarians into smaller pieces and allowing them to regenerate. Planarians were starved for 1 wk before experiments.

Bioinformatics and Cloning

Smed-ift88, *Smed-kif3a*, *Smed-fap22(qilin)*, *Smed-ic2*, and *Smed-lc1* were identified using the *S. mediterranea* genome database (Robb *et al.*, 2008; SmedGD: http://smedgd.neuro.utah.edu/) with the respective homologous human and *Chlamydomonas* protein sequences as queries. Phylogenetic analysis was based on a CLUSTALW alignment of the predicted planarian protein sequences from SmedGD with the homologous protein sequences from other organisms. SMED-IFT88 was compared with human IFT88 (Q13099), zebrafish IFT88 (Q2VF28), *Caenorhabditis* OSM-5 (Q9N4Z9), *Trypanosoma* IFT88 (Q386Y0), *Chlamydomonas* IFT88 (P27766), and human BBS4 (Q96RK4), which has a similar domain structure to IFT88 and was used as the outgroup. SMED-IC2 was compared with human DNAI2 (Q9GZS0), zebrafish IC1 (XM_001343837.2), *Ciona* IC1 (Q2PEE4), *Drosophila* Dme1 (CG1571), *Chlamydomonas* IC2 (Q9FPW0) with human Gβ1 subunit (P62879), and *Chlamydomonas* IC1 (Q39578) as control sequences. SMED-LC1 was compared with human DNAL1 (Q4LDG9), zebrafish DNAL1 (Q6DHB1), *Ciona* DNAL1 (Q8T888), *Trypanosoma* LC1 (Q385K0), *Drosophila* LC1 (Q9V3Q0), and *Chlamydomonas* LC1 (Q9XHH2) using another leucine-rich repeat protein *Nicotiana* LRR protein 1 (Q0R4K1) as a control sequence.

To prepare the plasmids for RNAi, total planarian RNA was isolated using Trizol (Invitrogen, Carlsbad, CA) and first-strand cDNA was made using AMV reverse transcriptase (New England Biolabs, Beverly, MA). To synthesize the vectors for RNAi, fragments ranging from 250 to 500 base pairs from the *Smed-ift88*, *Smed-kif3a*, *Smed-fap22(qilin)*, *Smed-ic2*, and *Smed-lc1* cDNA open reading frames were amplified using the following primers: *Smed-ift88* forward, GCGCTCTAGAATGGGCCGATTTGAAGAAGC; *Smed-ift88* reverse, GCGCCTCGAGTCAGGCAGTCCCATATCCGTGTA; *Smed-kif3a* forward, GCGCTCTAGAATATGGACAAACTGGAACTGGTAA; *Smed-kif3a* reverse, GCGCCTCGAGTCTGATATGATTTTCTCCTTCTGC; *Smed-fap22(qilin)* forward, GCGCTCTAGATTGCTGAGTGCAATAGATCTGGCT; *Smed-fap22(qilin)* reverse, GCGCCTCGAGAGATGATGCGATCTCTCGGT; *Smed-ic2* forward, GCGCTCTAGAATTCCCGATGTCGAGCTTCGAGAA; *Smed-ic2* reverse, GCGCCTCGAGGGACCGGTTTATGCGTTACAGC; *Smed-lc1* forward, GCGCTCTAGATGGCTAAAGCAACTACAAT; and *Smed-lc1* reverse, GCGCCTCGAGCTCAAGGCAAGGCAGGTC.

The cDNA sequences were inserted into the XbaI/XhoI sites of plasmid L4440 (Timmons and Fire, 1998), flanked by two opposing T7 RNA polymerase promoters that mediate the synthesis of dsRNA upon induction.

RNA Interference

Inhibition of gene expression *via* double-stranded RNA (dsRNA)-mediated RNA-interference (RNAi) in *S. mediterranea* was achieved as described previously (Newmark *et al.*, 2003). Briefly cDNA fragments of the target genes were inserted into pL4440, and the resulting plasmids were then used to transform HT115 (DE3) *Escherichia coli* cells that are deficient in RNaseIII, which prevents the degradation of newly synthesized dsRNA (Timmons *et al.*, 2001). Transformed cells were grown in 4 ml 2×YT medium, supplemented with ampicillin (100 μg/ml) and tetracycline (50 μg/ml), at 37°C for 16 h. The culture was then diluted 1:10 in fresh, prewarmed 2×YT medium supplemented with ampicillin (100 μg/ml) and grown to $OD_{595} = 0.4$. Expression of dsRNA was then induced with 1 mM IPTG at 37°C for 2–3 h. A pellet corresponding to 2 ml of the induced bacterial culture was mixed with 50 μl of liver homogenate, and 1 μl of red food dye was added to the artificial food mix to monitor the course of the feeding. Animals were allowed to feed on the artificial food mix for 1 h before being transferred to fresh medium. This regimen was repeated every 3 days for a total of four feedings. After 15–20 d animals were sampled to assess mRNA levels of targeted genes. When the majority of animals in the group displayed a phenotype, we proceeded to analyze cilia formation and the potential impact on the organism's physiology.

Semi-quantitative RT-PCR and Northern Blotting

Total RNA from two to three animals of ~10–20 mm in length was isolated using Trizol (Invitrogen) following the manufacturer's recommendations. Two micrograms of purified RNA was used to set up a 10-μl first-strand cDNA synthesis reaction with cloned AMV reverse transcriptase (New England Biolabs). PCR amplification was carried out with essentially the same primers that were used to make the RNAi vectors, and the number of cycles was optimized using primers for actin, in addition to non-targeted *Smed-ift88*, *Smed-ic2*, and *Smed-lc1*, as internal controls. PCR products were resolved in agarose gels and stained with ethidium bromide. Gels were digitized using a gel imaging system (Alpha Innotech, San Leandro, CA). Northern blot analysis was performed with 15 μg of total RNA resolved in a denaturing polyacrylamide gel, transferred to nylon membrane, and hybridized using our standard methods (King and Patel-King, 1995). Signals were detected using x-ray film (Fuji Photo Film, Tokyo, Japan) that was subsequently digitized using an ImageQuant LAS 4000 imager (GE Healthcare, Waukesha, WI). Final images were edited using Photoshop CS4 (Adobe Photo Systems, San Jose, CA); brightness and contrast were normalized using the auto-levels function.

Histochemistry and Immunofluorescence

Flatworms were fixed in relaxant solution (1% HNO_3, 0.85% formaldehyde, 50 mM $MgSO_4$; Dawar, 1973) at room temperature for 24 h in order to dissolve the mucus and to allow fixation to reach completion. Samples for histochemistry were embedded in paraffin wax, sectioned, and counterstained with hematoxylin and eosin following standard protocols. Sections were visualized under bright-field optics with an Olympus BX51 epifluorescence microscope (Olympus America, Melville, NY), equipped with PlanApo 60×/1.4 NA and 100×/1.35 NA oil immersion lenses. Images were acquired using a Magnafire cool-CCD digital camera (Optronics, Goleta, CA). Samples for immunofluorescence were briefly washed with phosphate-buffered saline (PBS), pH 7.2, and postfixed with freshly made 4% paraformaldehyde in PBS, pH 7.2. Fixed samples were permeabilized with 1% Igepal CA-630 (Sigma, St. Louis, MO) in PBS, pH 7.2, for 10 min and blocked with 3% normal goat serum, 1% BSA, 1% cold-water-fish gelatin, 0.1% Igepal CA-630, and 0.05% Tween-20 in PBS, pH

7.2. All antibodies used for immunofluorescence were diluted in PBS buffer containing 1% BSA, 0.1% cold-water-fish gelatin, and 0.05% Tween-20. Samples were treated with a 1:100 dilution of primary antibody against α-tubulin (clone B-5-1-2, Sigma) for 16 h at 4°C, washed with four changes of PBS, and incubated with Alexa Fluor 488–conjugated anti-mouse secondary antibody (Invitrogen) for 1 h. Samples were mounted whole on glass slides using a glycerol-based mounting medium containing DABCO (Sigma) as an anti-fade agent. Parafilm spacers were used to preserve the integrity of the body before placing a coverslip on top. Stained cilia on the lateral edges of the head region or on the ventral surface were visualized with an LSM 510 confocal microscope (Zeiss, Thornwood, NY) using a Fluor 40×/1.3 NA or Plan Apochromat 63× 1.4 NA oil immersion lens. Final images were edited using Photoshop CS4 (Adobe).

Electron Microscopy

For transmission electron microscopy (TEM) planarians were fixed at room temperature in 1% glutaraldehyde in PBS, pH 7.2, for 15 min and then changed into 1% glutaraldehyde in 0.1 M sodium cacodylate, pH 7.2, for 50 min. Samples were postfixed with 1% osmium tetroxide in 50 mM sodium cacodylate at room temperature. Fixed samples were stained en bloc with 1% uranyl acetate, dehydrated, and embedded in Epon.

For scanning electron microscopy (SEM), planarians were prefixed at room temperature with relaxant solution for 16 h and then fixed with 2.5% glutaraldehyde in 0.1 M sodium cacodylate, pH 7.4 (EM Science, Gibbstown, NJ) for 24 h at 4°C. Samples were postfixed at room temperature with 1% osmium tetroxide for 1 h, in the dark, and dehydrated through a series of ethanol solutions. Dehydrated flatworms were dried with an Autosamdri-815, Series A critical point dryer (Tousimis Research, Rockville, MD) and mounted with carbon tape and colloidal silver paint. Samples were sputter-coated with a Cressington 208 HR sputter coater (Ted Pella, Irvine, CA) before imaging with a Quanta 200 FEG scanning electron microscope (FEI, Sunnyvale, CA).

High-Speed Video Microscopy

Live planaria were placed on coverslips and confined in place using parafilm spacers. Beating cilia on the lateral sides of the head region were visualized with an Olympus BX51 microscope (Olympus America) under differential interference contrast (DIC) optics, and video was captured with an X-PRI F1 high frame-rate digital camera, capable of acquiring up to 1000 frames per second (AOS Technologies, Baden Daetwil, Switzerland). Video segments were acquired at 250 frames/s and edited using Virtualdub (www.virtualdub.org). Videos were decompiled, areas of interest were cropped, brightness and contrast levels were adjusted, and kymographs were produced from line scans perpendicular to the row of cilia using NIH ImageJ software as described previously (http://rsbweb.nih.gov/ij/; Dentler *et al.*, 2009). The same method was used to measure CBF under viscous loading; however, in this case the culture medium was supplemented with Ficoll (type 400; ~400,000 kDa molecular mass; Sigma) to final concentrations of 4, 8, and 16% wt/vol. The viscosity of the medium (in centipoise) was determined at 23°C using a calibrated Cannon-Fenske viscometer (size 25; no. 13-617A; Thermo-Fisher Scientific, Waltham, MA).

Gliding Assays

Groups of live planaria were placed in Petri dishes with fresh medium and left for at least 24 h under normal room lighting to acclimate. Movement of planarians was recorded with a MiniVID digital camera (LW Scientific, Lawrenceville, GA) fitted with a macro lens. Video segments were decompiled and the distance covered by each individual flatworm was measured using Metamorph (MDS Analytical Technologies, Sunnyvale, CA). Overlays of sequential movie frames, depicting the tracks of individual animals, were produced using Photoshop CS4 (Adobe).

RESULTS

Morphology, Distribution, and Physical Properties of Cilia in Planarians

S. mediterranea has been used extensively in recent years for research into stem cell biology and regeneration due in part to a sequenced genome and genetic tractability (Newmark and Sánchez Alvarado, 2002). To evaluate the use of *S. mediterranea* (Figure 1a) as an experimental model for the study of ciliary motility and the mechanisms of metachronal synchrony in a multiciliated epithelium, we initially characterized the structure and distribution of the cilia and investigated the role of these organelles in planarian physiology. The epithelium surrounding the planarian body is simple cuboidal with the nuclei of the cell monolayer aligned on a single level and in close proximity to the basal lamina (Figure 1b). We observed distinctive differences between the dorsal and ventral regions of the planarian epithelium. Cells on the ventral surface are cubical in shape and possess multiple motile cilia in contrast to the cells on the dorsal surface that are mostly nonciliated and more columnar (Figure 1b). Also present in the epithelium are rhabdites and secretory ducts that extend through the basement lamina to the epidermis from parenchymal secretory cells, as described previously (Bowen and Ryder, 1974; Hori, 1978). These structures secrete the mucus layer on which the flatworm is able to glide (Martin, 1978). The border between the ciliated and nonciliated epidermis extends to the lateral sides of the planarian body allowing several rows of cilia to be visible when the animal is viewed from the top (Figure 1c).

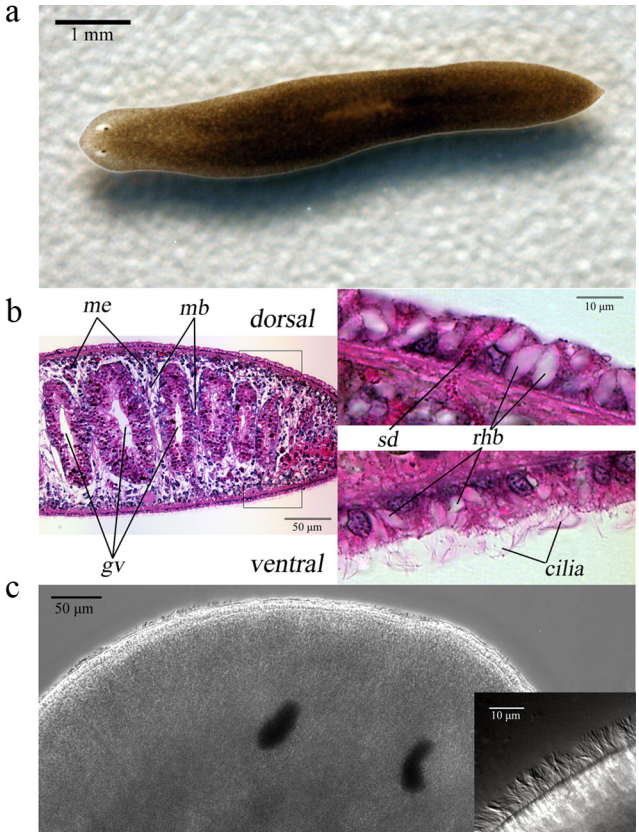

Figure 1. *S. mediterranea*: an experimental model for ciliated epithelia. (a) A typical *S. mediterranea* adult flatworm used in this study. (b) Cross section of paraffin-embedded planarian tissue counterstained with hematoxylin and eosin. Dorsoventral muscle bands (mb) divide the body into compartments that are traversed by branches of the gastrovascular (gv) cavity. The mesenchyme (me) of the planarian body is populated with numerous undifferentiated pluripotent cells, known as neoblasts. The epidermis consists of a simple cuboidal epithelium, composed of ciliated (ventral) or mostly nonciliated (dorsal) cells. Dispersed throughout the epithelium are secretory ducts (SD) and rhabdites (rhb); rhabdites in the dorsal surface appear larger in size. (c) Dorsal view of a live planarian. Motile cilia are readily visible on the lateral sides of the head region. The inset at right shows a magnified area of the left lateral side of the head where a row of cilia may be seen.

SEM confirmed that the entire ventral epithelium of *S. mediterranea* is ciliated (Figure 2a). These cilia appear homogenous in length (~10 μm); however, the number of cilia per unit surface area is larger at the head compared with other regions of the body (Figure 2a). In contrast, the dorsal surface is almost completely devoid of cilia with only small

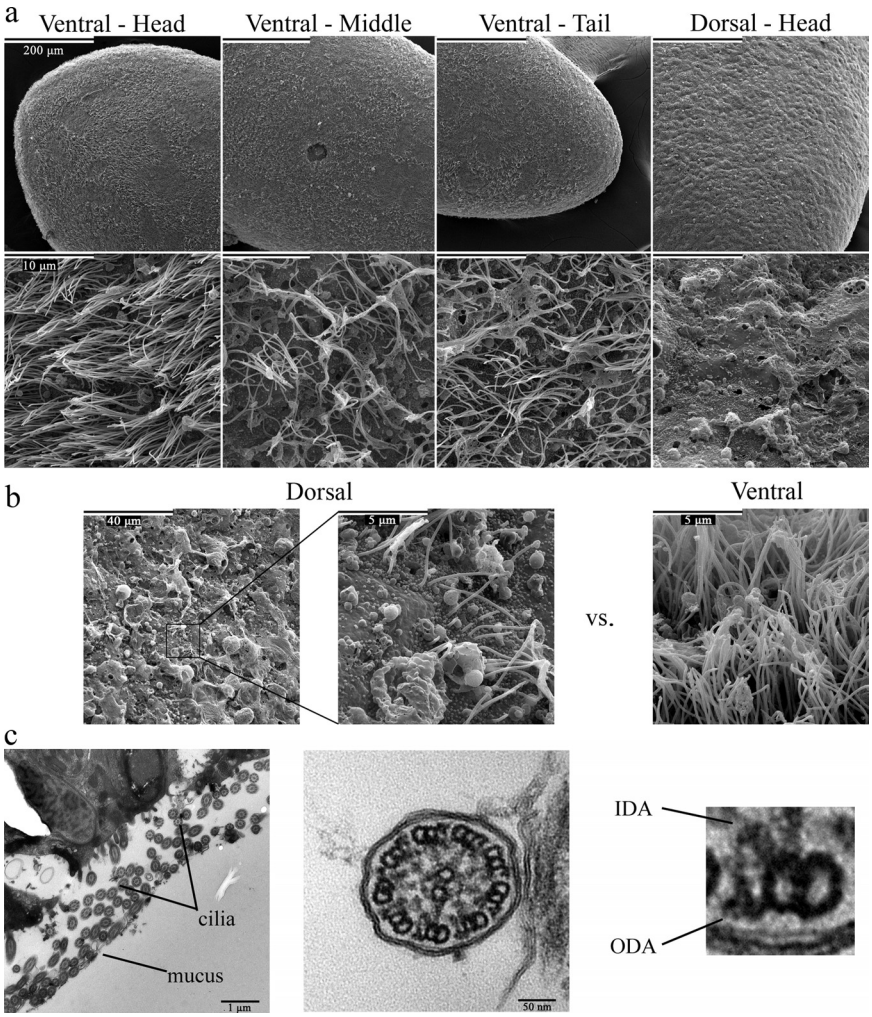

Figure 2. Distribution and structure of planarian cilia. (a) SEMs from different regions of the planarian epidermis at 500× (top panels) and 10,000× (bottom panels) magnification. The epithelium that lines the ventral surface is populated with cilia ~10 μm in length; however, the number of cilia per unit area is 5–10-fold larger around the head region compared with the middle and tail sections of the planarian body. In contrast, the entire dorsal surface appears uniform and largely devoid of cilia. Openings on the surface of the epithelium, between the rows of cilia, reveal the sites of mucus secretion. (b) SEMs showing clusters of cilia-like structures found on regions of the dorsal epithelium. A representative view of the dorsal epithelium at 2500× (left) and 20,000× (middle) magnification, reveals a single row of cilia, of various lengths. For comparison, an equivalent area of the ventral epithelium is shown (right). (c) TEMs of cross sections of planarian cilia. These organelles contain a 9+2 microtubule axoneme, radial spokes, and outer (ODA) and inner (IDA) dynein arms.

loci around the head region bearing clusters of cilia (Figure 2b). These cilia vary in size and appear to have sensory functions (MacRae, 1967; Bowen and Ryder, 1974). Numerous pores are also present on the surface of the epidermis, and represent the sites from which mucus is excreted. Transmission electron microscopy revealed that planarian cilia consist of a 9+2 microtubular axoneme with associated radial spokes, outer and inner dynein arms, and prominent projections emanating from the central pair microtubules (Figure 2c). We also often observed intradoublet microtubule structures located within the lumen of the A-tubule near the A-/B-tubule junction (these are readily evident in Figure 6b control).

To investigate the physical properties of planarian ciliary motility, we used high-speed video microscopy to visualize the cilia on the lateral sides of the head. We found that all cilia are motile and beat continuously even when the animal is stationary. Analysis of sequential frames from movies captured at 250 frames per second, revealed that the duration of a complete beat cycle is ~35–45 ms, which represents a CBF of ~24 Hz (Figure 3, a and b; Movie S1). The ciliary waveform is highly asymmetric, consisting of an effective and a recovery stroke (Figure 3c), similar to the waveform of cilia in epithelia from other organisms. The effective stroke represents one-third of the beat cycle and takes ~15 ms to complete, with the recovery stroke lasting for ~25 ms. Planarian ventral cilia beat in a coordinated manner and form metachronal waves with a mean wavelength of ~50 μm (Figure 3d), that are propagated along the direction of the effective stroke. All the cilia that we were able to visualize live, mostly around the head region, orient their beating along the same axis with the effective stroke directed toward the tail; this is consistent with their proposed role in driving gliding locomotion.

Cilia Are Required for Gliding Locomotion

Comparative analysis of the *S. mediterranea* genome revealed a great number of highly conserved genes with known ciliary function. To study the role of individual proteins in ciliary motility, we used RNAi to inhibit the expression of genes that are known to be essential for cilia formation. Using the *S. mediterranea* Genome Database (SmedGD; Robb *et al.*, 2008), we identified a conserved gene that encodes the IFT protein IFT88 (Figure 4a). IFT88 is a component of IFT complex B, and mutations that affect the normal levels of this protein result in short or diminished cilia (Marszalek *et al.*, 1999; Pazour *et al.*, 2000). A sequence of 527 base pairs from the coding region of *Smed-ift88* was inserted into plasmid L4440 (Timmons *et al.*, 2001) to produce the vector for RNAi. Groups of planarians were fed with bacteria expressing *Smed-ift88(RNAi)* or an empty vector, twice a week over a period of 2 wk; at which time a significant drop in mRNA was achieved, as evidenced by semi-quantitative RT-PCR

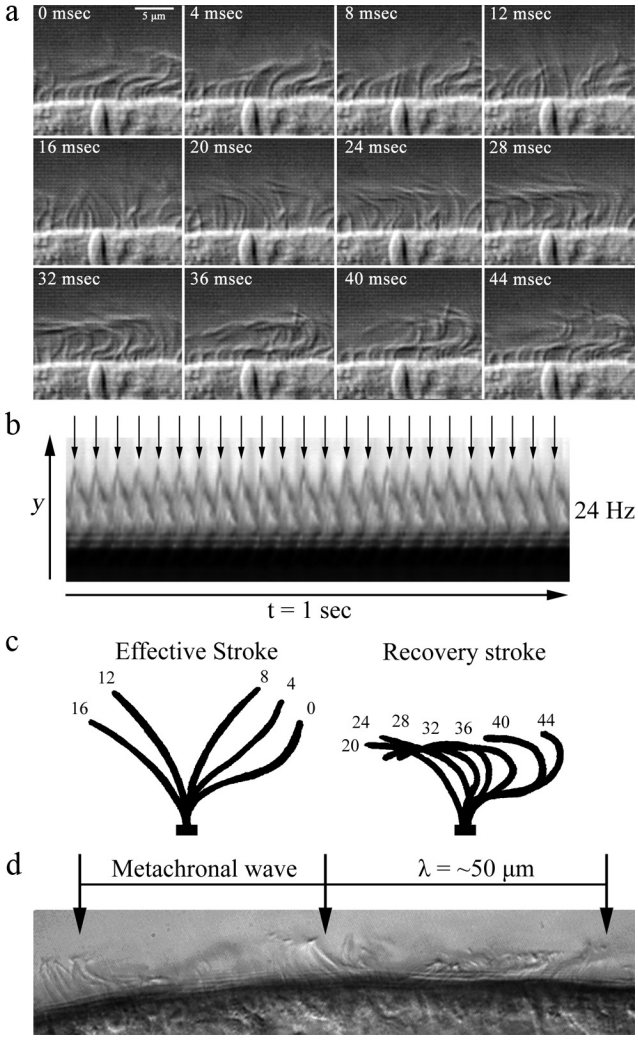

Figure 3. Physical properties of planarian ciliary motility. Assessment of planarian ciliary beat frequency and waveform by high-speed video microscopy captured at 250 frames/s using DIC optics. (a) Sequential frames (4 ms apart) of planaria cilia undergoing a single beat cycle. Cilia complete a full beat cycle in 35–45 ms (~24 Hz; also see Movie S1). Neighboring cilia synchronize their beating and form metachronal waves that are propagated along the plane of the ciliary beat. (b) Kymograph from the decompiled video of beating cilia over a 1-s period, illustrating 24 successive ciliary beat cycles. (c) Traces of a single cilium depicting its position at 4-ms intervals during a complete beat cycle. Planarian cilia beat with an asymmetric waveform consisting of an effective and a recovery stroke; the effective stroke is completed in ~15 ms representing one-third of the ciliary beat cycle. (d) A single video frame depicting the formation of metachronal waves from the coordination of neighboring cilia. The wavelength of the metachronal wave is ~50 μm.

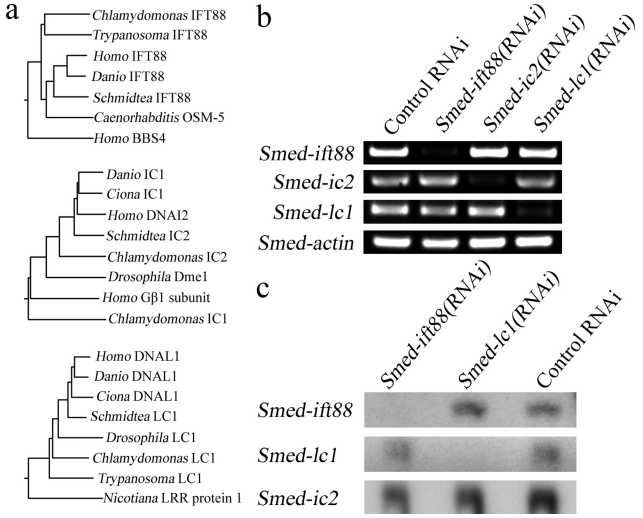

Figure 4. Reduction of ciliary gene expression in planarians by RNAi. (a) Neighbor-joining trees based on CLUSTALW alignments showing the relationship of SMED-IFT88, SMED-IC2 and SMED-LC1 with homologous proteins from other organisms. (b) Semi-quantitative RT-PCR to assess *Smed-ift88*, *Smed-ic2*, and *Smed-lc1* mRNA levels after treatment with the RNAi-inducing vectors. Actin mRNA was used as a control. (c) Northern blot analysis of *Smed-ift88*, *Smed-lc1*, and *Smed-actin* mRNA in RNAi- and control-treated animals. The reduction in mRNA levels is specific to the targeted gene and validates the RT-PCR data.

and verified by Northern blot analysis (Figure 4, b and c). Both DIC microscopy and confocal imaging of animals prepared for tubulin immunofluorescence revealed that the ventral surface of *Smed-ift88(RNAi)* animals was almost completely devoid of cilia, whereas cilia on flatworms that were fed with the empty vector remained essentially unchanged (Figure 5a).

Next, we investigated the potential impact of diminished ciliary assembly on the ability of the organism to move on solid substrates. Measurements of gliding velocity by means of live video microscopy showed that *Smed-ift88(RNAi)* flatworms moved significantly slower compared with controls (~0.46 vs. ~1.47 mm/s; Figure 5, b and c, and Movie S2). Furthermore, close examination revealed that the general mode of movement had drastically changed when compared with the control group or wild-type animals. Specifically, *Smed-ift88(RNAi)* animals displayed no gliding locomotion and relied almost exclusively on peristaltic movements of their muscles to essentially squeeze themselves across the substrate (Figure 4d and Movies S3 and S4). Targeting of other conserved genes that are also essential for cilia formation including *Smed-kif3a* and *Smed-fap22(qilin)* yielded similar results (data not shown). These observations are in agreement with other recent studies (Rink *et al.*, 2009) and provide direct evidence that cilia are required for gliding-based movement in planarians.

Outer Arm Dynein Is Required for Metachronal Wave Formation and Gliding Locomotion

We next used RNAi to reduce expression of integral components of the outer dynein arm that are required for the structural integrity of the complex (IC2/DNAI2) or are involved in its regulation (LC1/DNAL1; Figure 4a). IC2 is a WD-repeat IC located at the base of the motor unit and is essential for the assembly of the entire outer arm complex onto the axoneme (Kamiya, 1988; Mitchell and Kang, 1991). Defects in the genes that encode IC2 cause a significant drop in CBF in *Chlamydomonas* and are responsible for primary ciliary dyskinesia type 9 (CILD9; OMIM: 612444) in humans (Loges *et al.*, 2008). LC1 is a light chain that in *Chlamydomonas* axonemes tethers the motor unit of the outer arm γ HC to the A-tubule of the outer doublets. LC1 plays an important role in outer arm activity during conformational switching (Patel-King and King, 2009).

To study the loss-of-function effects of *Smed-ic2* and *Smed-lc1*, we constructed specific RNAi vectors that were used to

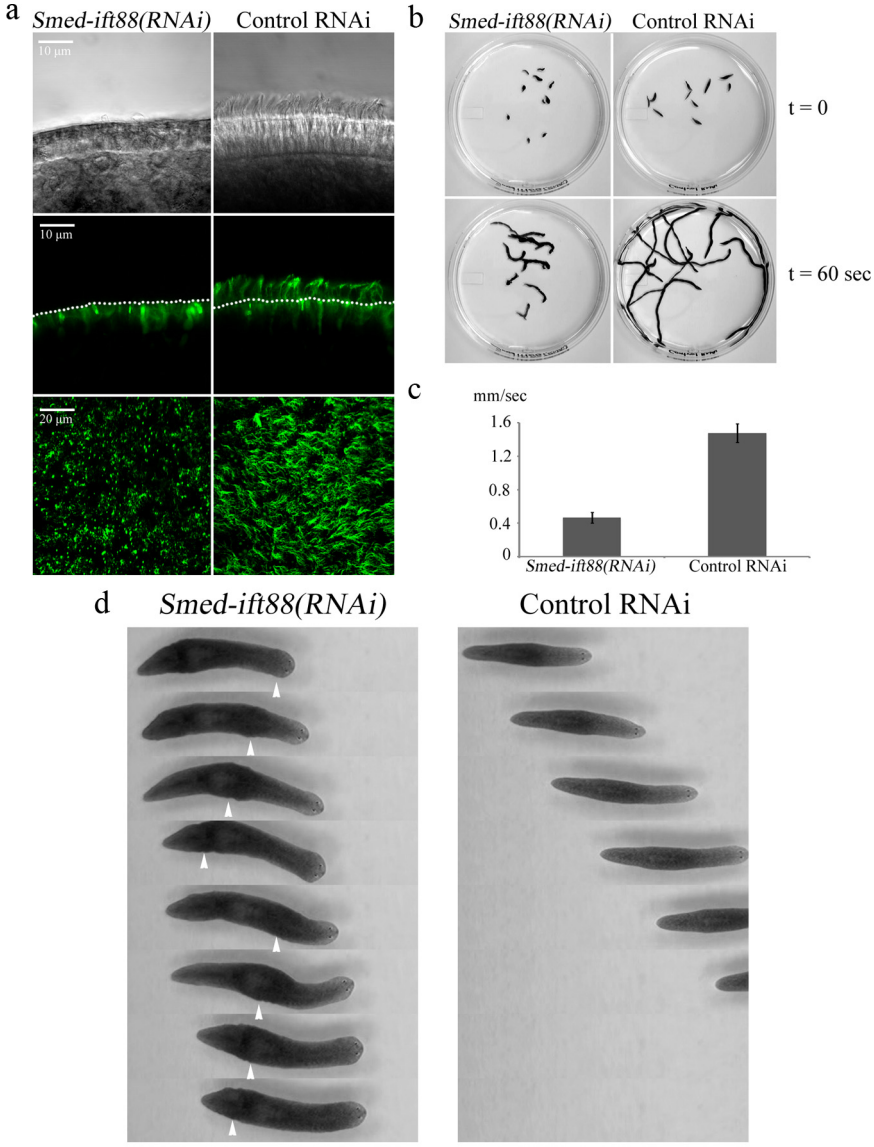

Figure 5. Cilia are required for gliding locomotion in planarians. (a) Cilia from *Smed-ift88(RNAi)* and control-treated animals were observed using DIC optics (top panels). In addition, planaria were stained with anti-α-tubulin antibody (clone B-5-1-2) and visualized using confocal microscopy (side view, middle panel; top view, bottom panel). Analysis showed a substantial decrease in the number of cilia in the *Smed-ift88(RNAi)* flatworms compared with control. The dotted lines in the middle panels mark the apical surface of the ventral epithelium. The numerous bright puncta visible on the ventral surface of *Smed-ift88(RNAi)* animals derive from nonspecific binding of the secondary antibody to mucus associated with the gland cells. (b) Initial frame (t = 0; top panel) and overlays of sequential frames (t = 60 s; bottom panel) from 60-s video segments, illustrating the distance traveled by individual flatworms in *Smed-ift88(RNAi)* and control-treated groups. (c) Quantification of gliding velocity in RNAi- and control-treated animals. *Smed-ift88(RNAi)* animals moved at ~0.46 mm/s (n = 23, sem = 0.013) compared with ~1.47 mm/s (n = 27, sem = 0.02) for the control group. (d) Sequential video frames (1.5 s apart) illustrating the differences in the general mode of movement between *Smed-ift88(RNAi)* and control-treated animals. *Smed-ift88(RNAi)* flatworms display no gliding locomotion and travel using peristaltic muscular movements. Arrowheads show peristaltic muscular waves as they propagate along the body (also see Movies S3 and S4).

effectively inhibit expression of both genes (Figure 4b). DIC microscopy and confocal immunofluorescence analysis revealed that cilia on the *Smed-ic2(RNAi)* and *Smed-lc1(RNAi)* animals were similar in number and appearance to those of control-fed animals, which is consistent with the predicted function of both these genes (Figure 6a). TEM cross sections revealed that *Smed-ic2(RNAi)* cilia were either completely lacking outer arms, or the densities that correspond to these complexes were significantly reduced compared with controls (Figure 6b, top and middle panels). This is consistent with an outer arm assembly defect as reported previously (Kamiya and Okamoto, 1985; Mitchell and Rosenbaum, 1985). In contrast, *Smed-lc1(RNAi)* cilia had axonemes with intact outer dynein arms, and these structures appeared virtually indistinguishable from those in cilia of control-fed animals (Figure 6b, top and bottom panels). Thus, unlike trypanosomes (Baron *et al.*, 2007), reduction of LC1 in *S. mediterranea* does not result in the failure of outer arm assembly.

The *Smed-ic2(RNAi)* and *Smed-lc1(RNAi)* planaria moved at ~0.39 and ~0.44 mm/s, respectively, compared with ~1.47 mm/s for the control group (Figure 7a). This rate is essentially similar to that seen for the *Smed-ift88(RNAi)* animals, which completely lack cilia. Furthermore, these outer arm–deficient animals displayed an almost identical locomotion phenotype to that described above, using muscular contractions to power their movement (Movies S5 and S6).

To investigate the underlying cause of diminished gliding locomotion and the specific effects of impaired outer arm dynein activity, we used high frame-rate video microscopy to analyze the waveform and beat frequency of cilia in *Smed-ic2(RNAi)* and *Smed-lc1(RNAi)* animals. We found that although the waveform remained apparently unchanged, the beat frequency was significantly reduced compared with control: *Smed-ic2(RNAi)* and *Smed-lc1(RNAi)* cilia both beat at ~10 Hz (Figure 7b and Movie S7). Significantly, cilia on both *Smed-ic2(RNAi)* and *Smed-lc1(RNAi)* animals failed to coordinate their beating. As a result neighboring cilia beat in completely different phases and did not form metachronal waves. (Figure 7c and Movie S7).

To test whether the creation of metachronal waves specifically required the outer arms or depended simply on the CBF and/or the ratio between the cilia power output and the

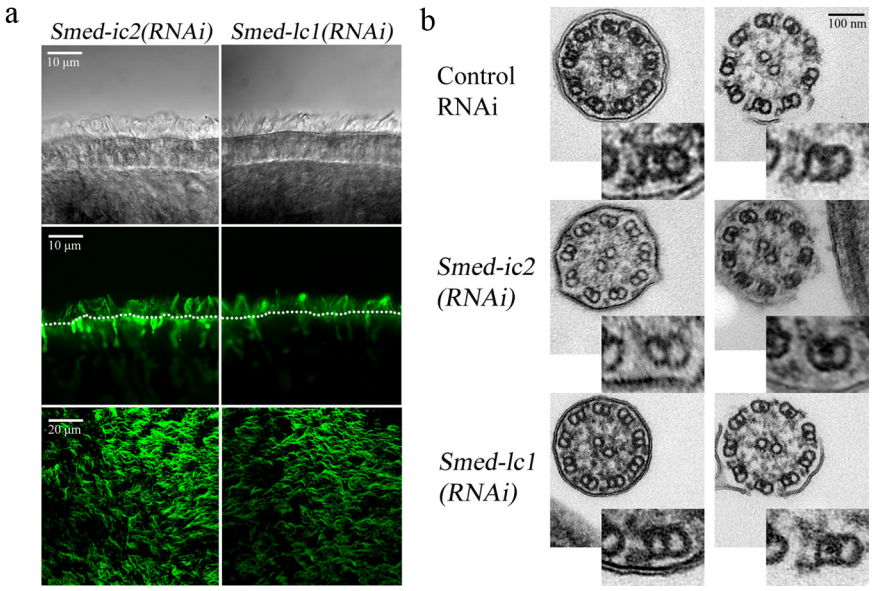

Figure 6. *Smed-lc1* is not required for outer arm dynein assembly. (a) DIC (top panel) and confocal (side view, middle panel; top view, bottom panel) images of cilia stained with the anti-α-tubulin antibody from *Smed-ic2(RNAi)* and *Smed-lc1(RNAi)* animals. The number and organization of cilia appears normal. Dotted lines mark the apical surface of the ventral epithelium. (b) TEMs of cross sections from cilia with complete (left) or disrupted membranes (right), taken from *Smed-ic2(RNAi)*, *Smed-lc1(RNAi)* and control-treated animals. The insets at the bottom right corner of each micrograph show a magnified view of a single microtubule doublet where the presence or absence of dynein arm complexes can be more readily evaluated. Assembly of outer arm dynein complexes is largely disrupted in *Smed-ic2(RNAi)* animals, whereas in *Smed-lc1(RNAi)* cilia the outer arms appear intact and comparable to those of control-fed flatworms.

applied viscous force, we measured gliding locomotion and CBF in planarians under increased viscous load. Normally mucus-propelling cilia are surrounded by a low viscosity fluid known as periciliary liquid (PCL), and come in contact with the layer of mucus, which sits above the PCL a few micrometers from the surface of the tissue, only with their

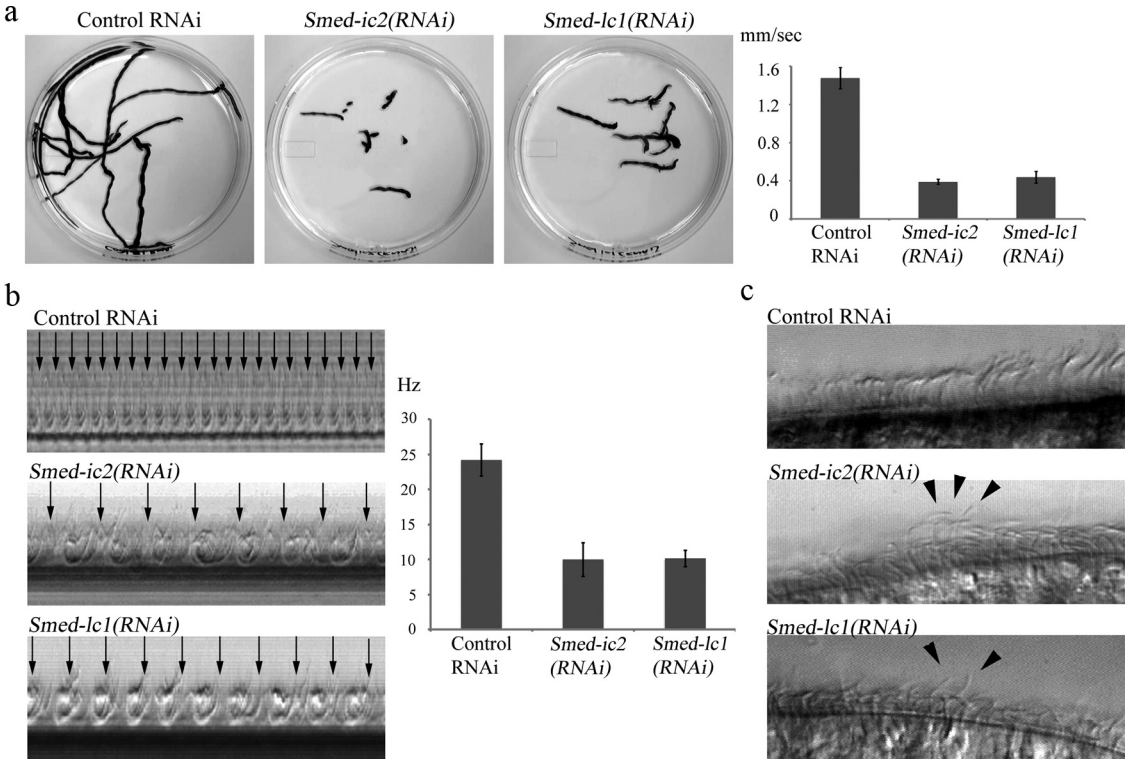

Figure 7. Metachronal synchrony of beating cilia requires outer arm dynein and *Smed-lc1*. (a) Overlay of sequential frames from 60-s video segments illustrating the distance traveled by individual planaria in *Smed-ic2(RNAi)*, *Smed-lc1(RNAi)*, and control-treated groups (left; also see Movies S2, S5, and S6). *Smed-ic2(RNAi)* and *Smed-lc1(RNAi)* flatworms moved at ~0.39 mm/s (n = 31, sem = 0.004) and ~0.44 mm/s (n = 29, sem = 0.011), respectively, compared with ~1.47 mm/s (n = 27, sem = 0.02) for the control group (right). (b) Kymographs of beating cilia from control-, *Smed-ic2(RNAi)*- and *Smed-lc1(RNAi)*-treated animals. Cilia of both *Smed-ic2(RNAi)* and *Smed-lc1(RNAi)* flatworms beat at ~10 Hz (n = 22, sem = 0.51) and ~10 Hz (n = 50, sem = 0.24) compared with ~24 Hz (n = 23, sem = 0.47) for the control. (c) Single video frames of beating cilia from control, *Smed-lc1(RNAi)* and *Smed-ic2(RNAi)* flatworms. Cilia of both *Smed-lc1(RNAi)* and *Smed-ic2(RNAi)* groups failed to synchronize their movement but rather beat continuously in different phases (also see Movie S7); consequently, metachronal waves do not form. Arrowheads show representative cilia from *Smed-ic2(RNAi)* and *Smed-lc1(RNAi)* flatworms that are in different phases of the beat cycle.

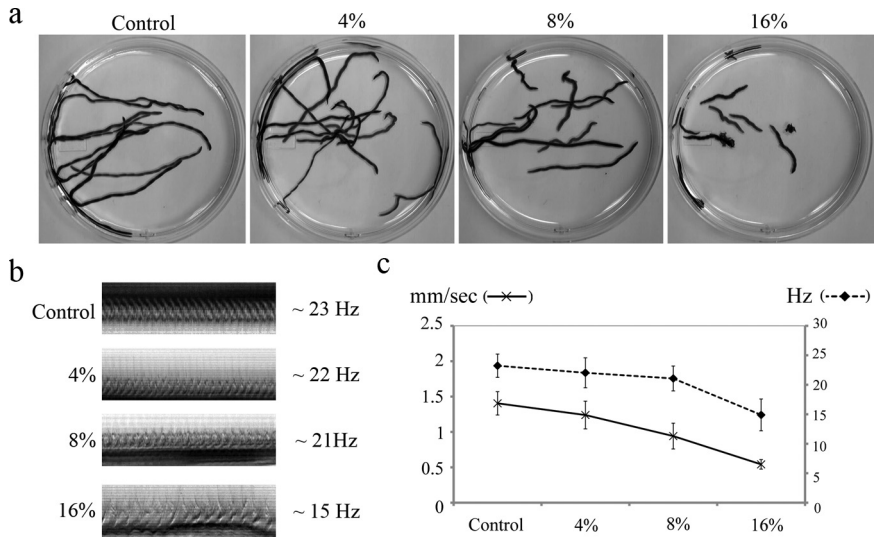

Figure 8. Effects of high viscous loads on CBF and gliding locomotion. (a) Overlay of sequential frames from 60-s video segments, illustrating the distance traveled by individual planaria in increasing concentrations of Ficoll (0, 4, 8, and 16%). (b) Kymographs of cilia beating in the presence of increasing concentrations of Ficoll. CBF decreased from ~23 Hz (n = 30, sem = 0.36) in 0% Ficoll to ~22 Hz (n = 31, sem = 0.45) in 4%, ~22 Hz (n = 28, sem = 0.39) in 8% and ~15 Hz (n = 28, sem = 0.51) in 16% Ficoll. (c) Graph depicting gliding velocity and CBF under varying viscous load. Gliding velocity decreased from ~1.4 mm/s (n = 20, sem = 0.03) in 0% Ficoll to ~1.24 mm/s (n = 20, sem = 0.04) in 4%, ~0.94 mm/s (n = 20, sem = 0.04) in 8% and ~0.54 mm/s (n = 20, sem = 0.016) in 16% Ficoll.

tips during the effective stroke (reviewed in Smith *et al.*, 2008; also see Figure 2c). Therefore, cilia are normally under load only during a fraction of their beat cycle. By increasing the viscosity of the bulk medium, we aimed to subject planarian cilia to a constant load in order to measure the effect on CBF and metachronal synchrony.

A group of wild-type animals were subjected to a series of media containing increasing concentrations of Ficoll, and their gliding velocity and ciliary motility was recorded by video microscopy (Figure 8). The velocity of planarian movement gradually decreased from ~1.4 mm/s in 0% Ficoll (viscosity = 1 cP; centipoise) to ~0.54 mm/s in 16% Ficoll (~12 cP; Figure 8, a and c). CBF remained relatively unchanged at viscosities up to ~4 cP and declined by ~30% (to ~15 Hz) at ~12 cP (Figure 8, b and c). Although gliding locomotion was almost completely impaired under high viscous load (~12 cP; Movie S8), the cilia beating in these viscous media were still able to coordinate their beat and form metachronal waves (Movie S9).

To further dissect the role of outer arm dynein and its regulatory subunit (LC1) in regulating the creation of metachronal waves, we performed a detailed analysis of ciliary beating in *Smed-ic2(RNAi)* and *Smed-lc1(RNAi)* animals as they compared with control. First, we constructed kymographs from multiple line scans along single rows of cilia (Figure 9a). Careful analysis of kymographs from *Smed-ic2(RNAi)* and *Smed-lc1(RNAi)* cilia revealed multiple peaks per beat cycle (Figure 9a), which we interpret as cilia in a single plane beating off-phase. In contrast, kymographs produced from control animals consistently displayed a single peak per beat cycle demonstrating a tight coordination of the ciliary beating in neighboring cilia. Averaging the line scans along a single row of cilia to produce compound kymographs resulted in loss of distinguishable peaks in *Smed-ic2(RNAi)* and *Smed-lc1(RNAi)* cilia due to off-phase beat cycles of neighboring cilia being averaged out. Conversely, compound kymographs from control animals displayed clear peaks, similar to those from single line scans. It should be noted that the different peaks observed in kymographs from *Smed-ic2(RNAi)* and *Smed-lc1(RNAi)* cilia displayed similar periodicity suggesting that there is no significant variation in the duration of the beat cycle between neighboring cilia.

To test whether the outer arm dynein has a specific role in coordinating ciliary beating or if the loss of metachronal waves in *Smed-ic2(RNAi)* and *Smed-lc1(RNAi)* animals is merely the result of a wide temporal variation in the beat cycle of neighboring cilia due to impaired outer arm activity, we analyzed the beat of individual cilia. Because it is not feasible to study planarian cilia in isolation, we randomly selected individual cilia from rows of neighboring cilia and measured their beat frequency by means of high-speed video microscopy. For *Smed-ic2(RNAi)* and *Smed-lc1(RNAi)* cilia we obtained a mean beat frequency of 10.06 and 9.58 Hz with an SD of 2.18 and 2.06 Hz, respectively (Figure 9b). In comparison, cilia from control animals beat with a mean frequency of 22 Hz and an SD of 2.54. Plotting the normal distributions of the recorded beat frequencies demonstrated no significant temporal variability in the beat cycle of *Smed-ic2(RNAi)* and *Smed-lc1(RNAi)* cilia compared with control (Figure 9c). We also quantified the number of cilia that were stalling at any given point through their beat cycle. Less than 10% of the cilia from *Smed-ic2(RNAi)* and *Smed-lc1(RNAi)* animals were found to be stalling (Figure 9d). The relatively small number of stalling cilia in *Smed-ic2(RNAi)* and *Smed-lc1(RNAi)* flatworms can likely be attributed to the spatial constraints induced by cilia in close proximity beating off-phase.

DISCUSSION

Metachronal Synchrony of Beating Cilia

Motile cilia in epithelial tissues mediate the continuous transport/clearance of mucus and other peri-ciliary fluids. To perform these tasks, cilia are clustered together in large numbers and synchronize their beats, forming metachronal waves (e.g., Machemer, 1972; Eshel and Priel, 1987); however, the mechanism(s) by which these waves are governed are largely unknown. The prevailing view is that the metachronal coordination is, at least in part, the result of hydrodynamic coupling between neighboring cilia (Sleigh, 1974; Gheber and Priel, 1989). Because of the spatial constraints of a tightly packed ciliated epithelium, arrays of neighboring cilia achieve optimal energetic output by coordinating their beats to avoid interfering with each other's movement. Mathematical models have shown that metachronal synchrony of multiciliated systems is indeed energetically favorable and thus may arise spontaneously driven by hydrodynamic forces (Gueron and Levit-Gurevich, 1998; Sorin,

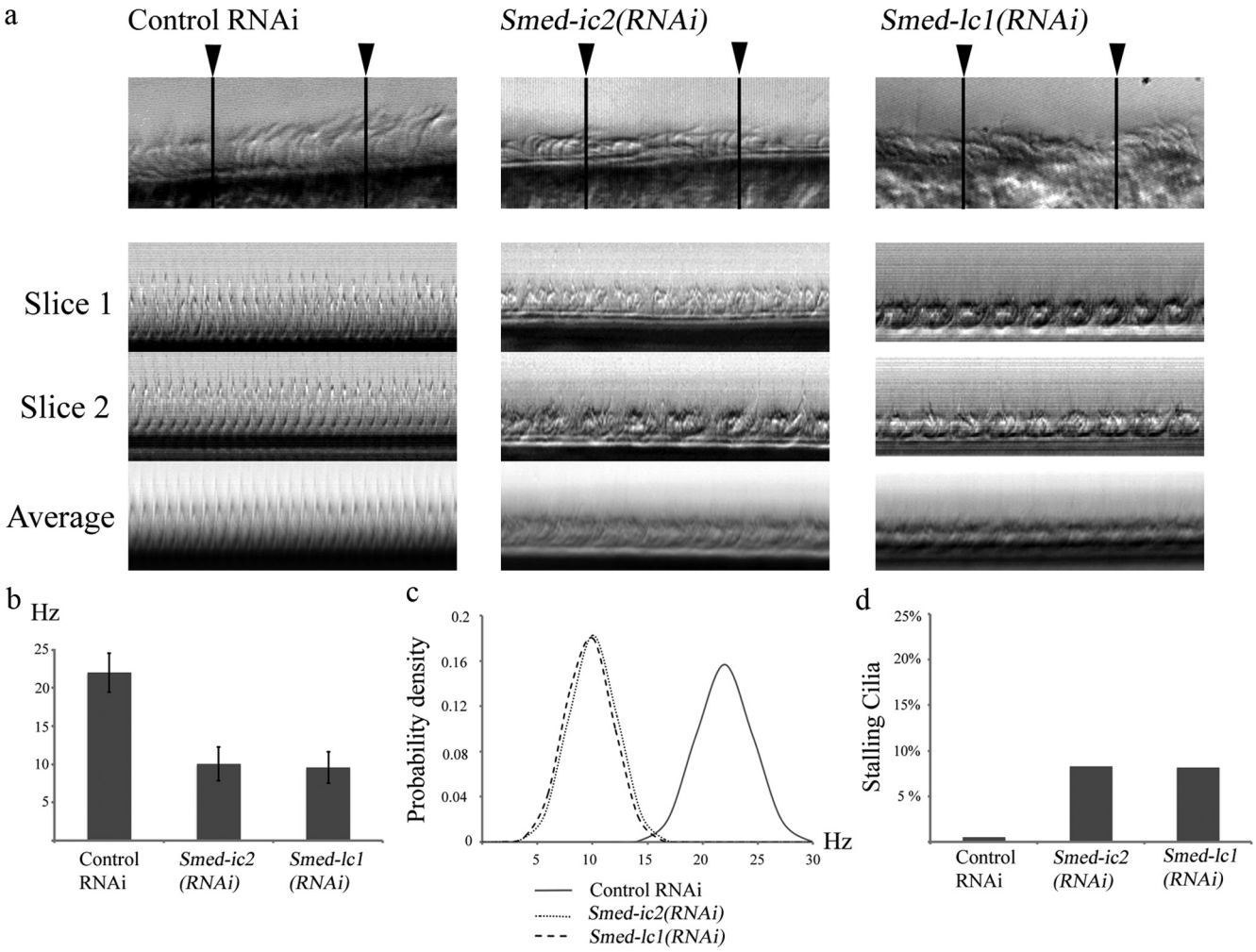

Figure 9. Variability in the ciliary beat cycle. (a) Kymographs constructed from line scans at two different sites along a row of cilia (indicated by the arrowheads; slice 1 and 2) and from averaging multiple line scans covering the entire field of view (average). Note the multiple peaks per beat cycle in *Smedic2(RNAi)* and *Smed-lc1(RNAi)* compared with single sharp peaks in the control. (b) CBF of individual cilia measured by high-speed video microscopy. Control cilia beat at ~22 Hz (n = 52, sem = 0.35) compared with ~10 Hz (n = 50, sem = 0.3) for *Smed-ic2(RNAi)* and ~9.6 Hz (n = 57, sem = 0.28) for *Smed-lc1(RNAi)*. (c) Normal distributions of beat frequency measurements of individual cilia from control, *Smed-ic2(RNAi)* and *Smed-lc1(RNAi)* cilia. The sample variance in the control is 6.46 compared with 4.77 and 4.25 for *Smed-ic2(RNAi)* and *Smed-lc1(RNAi)*. Thus lack of metachronal synchrony in the experimental animals is not due to increased variability in CBF (d) Percentage of stalling cilia in control (0.5%), *Smed-ic2(RNAi)* (8.25%) and *Smed-lc1(RNAi)* (8.12%) animals.

2007). The hydrodynamic hypothesis is further supported by observations on the effect of increased viscous loads on metachronal wave properties in *Paramecium* (Machemer, 1972) and on the spontaneous synchronization of flagellar oscillations of spermatozoa when they are placed in close proximity (Riedel *et al.*, 2005). Taken together these data support a model whereby hydrodynamic forces are sufficient to drive the formation of metachronal waves. However, maintenance of the synchrony must involve mechanical feedback from the cilia to ensure that the beats remain in-phase.

Numerous studies have described the response of cilia to various environmental stimuli. For example, cilia in murine and human airway epithelia are capable of increasing their CBF, and thus the rate of mucociliary clearance in response to specific compounds (Lorenzo *et al.*, 2008; Shah *et al.*, 2009). In addition, a link between external hydrodynamic forces on cilia and intracellular planar cell polarity signaling in ependymal cells was recently described (Guirao *et al.*, 2010). These observations imply that coordination of cilia and the formation of metachronal waves is not merely a passive mechanical response but involves active biochemical processes, regulated by elements of the ciliary machinery. Our data suggest that the LC1 conformational switch responds to the hydrodynamic forces exerted on the cilium by acting directly to modulate outer arm dynein activity and thus regulate the coordination of ciliary beating and ultimately the formation of metachronal waves. This model is complementary to the hydrodynamic coupling hypothesis and introduces a feedback mechanism by which cilia may sense their environment, relate this to the current mechanical state, and respond by actively regulating the physical properties of their beat until optimal efficiency is achieved.

The Role of Outer Arm Dynein in Metachronal Synchrony

The shape and frequency of the ciliary beat govern the characteristics of metachronal waves and determine the efficiency of fluid clearance. CBF is particularly important, as the generated force from ciliary activity appears to depend linearly on CBF (Teff *et al.*, 2008). CBF is controlled primarily

through the action of outer arm dynein motors (Kamiya and Okamoto, 1985; Mitchell and Rosenbaum, 1985; de Iongh and Rutland, 1995) and is regulated in response to different environmental and intracellular stimuli (Lorenzo *et al.*, 2008; Shah *et al.*, 2009). Here we demonstrate that *S. mediterranea* cilia lacking outer arm dynein are unable to coordinate their beat and form metachronal waves. However, the observed decrease in CBF in outer arm-less cilia does not alone account for the lack of metachronal synchrony because a comparable decline in the CBF of wild-type cilia placed in viscous media did not impair the formation of metachronal waves. In addition, the loss of metachronal coordination is unlikely to be induced by an increased variability in the duration of the beat cycle of cilia with impaired outer arm activity, as we measured no significant variability in the beating of dynein-deficient cilia compared with controls. Taken together these results suggest that outer arm dynein controls CBF and metachronal synchrony via separate mechanisms. Evidence that inner arm dyneins, which control waveform, are also important for metachronal synchrony came from analysis of *Tetrahymena* strains in which a single heavy chain (DYH7, which is equivalent to the I1/f βHC of *Chlamydomonas*) was knocked out (Wood *et al.*, 2007). Similarly, disrupting hydin within the central pair complex, which is involved in inner arm regulation also affects metachrony (Lechtreck *et al.*, 2008).

Previous studies have shown that under high viscous load there are significant changes in the wavelength and direction of metachronal waves (Gheber *et al.*, 1998) that can be attributed to alterations in the temporal asymmetry of the ciliary beat (Gheber and Priel, 1990). This would suggest the presence of a feedback mechanosensory system that responds to mechanical forces applied to the cilium by changing the properties of the beat. Such systems, which involve the outer arm dynein motor, have been previously described in the *C. reinhardtii* flagellum (Hayashibe *et al.*, 1997). Control of metachronal synchrony in response to hydrodynamic forces may represent an additional conserved function of outer arm dynein whereby the LC1 mechanosensitive regulatory subunit provides the necessary feedback to regulate this process.

LC1 as a Sensor of Hydrodynamic Interactions

LC1 is a leucine-rich–repeat protein and one of the most conserved subunits of the outer arm dynein complex (54% sequence identity between algal and human homologues; Kajava, 1998; Benashski *et al.*, 1999). In *Chlamydomonas*, two copies of LC1 bind directly to AAA domains of the γ HC motor unit (Benashski *et al.*, 1999; Wu *et al.*, 2000) and tether that motor domain to the A-tubule of the outer doublet microtubules. Expression of dominant-negative forms of LC1 caused adverse effects on swimming velocity, with the flagella beating constantly out-of-phase, and stalling near the power/recovery stroke switch point, suggesting that LC1 regulates outer arm dynein activity through a conformational switch (Patel-King and King, 2009).

To further dissect the role of LC1 in outer arm dynein function and to test whether it is involved in metachronal wave formation, we inhibited the expression of *Smed-lc1*. We observed that cilia lacking SMED-LC1 assembled a full complement of outer arms but exhibited a significant decrease in CBF and lost the ability to form metachronal waves. Similar RNAi studies in *Trypanosoma brucei* found that loss of LC1 resulted in reverse flagellar beat and backward swimming movement. However, these knockdown strains also had an outer arm assembly defect and mis-orientation of the central pair apparatus (Baron *et al.*, 2007). This suggested that the motility defects observed in LC1-deficient trypanosomes might be a secondary effect attributable to the lack of a normal complement of outer arm dynein motors and/or dysfunction of the central pair complex. Our data are consistent with observations on a *Chlamydomonas* mutant (*oda-2t*), which lacks the outer arm γ HC motor domain and LC1, and exhibits pronounced motility defects (Liu *et al.*, 2008). We propose that LC1 acts in a mechanosensory feedback mechanism controlling outer arm activity and thus the ciliary beat based on external conformational cues.

S. mediterranea *as a Model System for Ciliary Motility*

This study also has obvious implications for the use of *S. mediterranea* as a model organism for dissecting the biology of cilia and cilia-based motility. Specifically, the observation that ciliary function correlates with gliding ability in planarians provides an excellent platform for the screening, identification, and characterization of genes that play an important role in ciliary function. Additional advantages of *S. mediterranea* include a well-defined and easily accessible ciliated epithelium, a sequenced genome and established tools for manipulating gene expression, powerful assays to study the physical properties of ciliary motility, and the low cost of use and maintenance in the laboratory (Newmark *et al.*, 2003; Rompolas *et al.*, 2009).

ACKNOWLEDGMENTS

We thank Dr. B. R. Gravely for providing us with a founding colony of *S. mediterranea*, Dr. M. Smielewska for useful discussions, and Dr. G. Pazour and J. Follit (University of Massachusetts Medical School) for their help with the SEM experiments. This study was supported by Grant GM51293 from the National Institutes of Health to S.M.K.

REFERENCES

Afzelius, B. A. (2004). Cilia-related diseases. J. Pathol. *204*, 470–477.

Baron, D. M., Kabututu, Z. P., and Hill, K. L. (2007). Stuck in reverse: loss of LC1 in *Trypanosoma brucei* disrupts outer dynein arms and leads to reverse flagellar beat and backward movement. J. Cell Sci. *120*, 1513–1520.

Benashski, S. E., Patel-King, R. S., and King, S. M. (1999). Light chain 1 from the *Chlamydomonas* outer dynein arm is a leucine-rich repeat protein associated with the motor domain of the γ heavy chain. Biochemistry *38*, 7253–7264.

Bessen, M., Fay, R. B., and Witman, G. B. (1980). Calcium control of waveform in isolated flagellar axonemes of *Chlamydomonas.* J. Cell Biol. *86*, 446–455.

Bowen, I. D., and Ryder, T. A. (1974). The fine structure of the planarian *Polycelis tenuis* (Iijima). Protoplasma *80*, 381–392.

Cebria, F., and Newmark, P. A. (2005). Planarian homologs of netrin and netrin receptor are required for proper regeneration of the central nervous system and the maintenance of nervous system architecture. Development *132*, 3691–3703.

Dawar, B. L. (1973). A combined relaxing agent and fixative for Triclads (Planarians). Biotech. Histochem. *48*, 93–94.

de Iongh, R. U., and Rutland, J. (1995). Ciliary defects in healthy subjects, bronchiectasis, and primary ciliary dyskinesia. Am. J. Respir. Crit. Care Med. *151*, 1559–1567.

Dentler, W., Vanderwaal, K., and Porter, M. E. (2009). Recording and analyzing IFT in *Chlamydomonas* flagella. Methods Cell Biol. *93*, 145–155.

Dorey, A. E. (1965). The organization and replacement of the epidermis in acoelous Turbellarians. Q J. Microsc. Sci. *106*, 147–172.

Eshel, D., and Priel, Z. (1987). Characterization of metachronal wave of beating cilia on frog's palate epithelium in tissue culture. J. Physiol. *388*, 1–8.

Fliegauf, M., Benzing, T., and Omran, H. (2007). When cilia go bad: cilia defects and ciliopathies. Nat. Rev. Mol. Cell Biol. *8*, 880–893.

Gheber, L., Korngreen, A., and Priel, Z. (1998). Effect of viscosity on metachrony in mucus propelling cilia. Cell Motil. Cytoskelet. *39*, 9–20.

Gheber, L., and Priel, Z. (1989). Synchronization between beating cilia. Biophys. J. *55*, 183–191.

Gheber, L., and Priel, Z. (1990). Ciliary activity under normal conditions and under viscous load. Biorheology *27*, 547–557.

Gu, W., Sander, T., Heils, A., Lenzen, K., and Steinlein, O. (2005). A new EF-hand containing gene EFHC2 on Xp11.4, tentative evidence for association with juvenile myoclonic epilepsy. Epilepsy Res. *66*, 91–98.

Gueron, S., and Levit-Gurevich, K. (1998). Computation of the internal forces in cilia: application to ciliary motion, the effects of viscosity, and cilia interactions. Biophys. J. *74*, 1658–1676.

Guirao, B., *et al*. (2010). Coupling between hydrodynamic forces and planar cell polarity orients mammalian motile cilia. Nat. Cell Biol. *12*, 341–350.

Habermacher, G., and Sale, W. S. (1997). Regulation of flagellar dynein by phosphorylation of a 138-kD inner arm dynein intermediate chain. J. Cell Biol. *136*, 167–176.

Hasegawa, E., Hayashi, H., Asakura, S., and Kamiya, R. (1987). Stimulation of *in vitro* motility of *Chlamydomonas* axonemes by inhibition of cAMP-dependent phosphorylation. Cell Motil. Cytoskelet. *8*, 302–311.

Hayashibe, K., Shingyoji, C., and Kamiya, R. (1997). Induction of temporary beating in paralyzed flagella of *Chlamydomonas* mutants by application of external force. Cell Motil. Cytoskelet. *37*, 232–239.

Hori, I. (1978). Possible role of rhabdite-forming cells in cellular succession of the planarian epidermis. J. Electron Microsc. *27*, 89–102.

Hyams, J., and Borisy, G. (1978). Isolated flagellar apparatus of *Chlamydomonas*: characterization of forward swimming and alteration of waveform and reversal of motion by calcium ions *in vitro*. J. Cell Sci. *33*, 235–253.

Ibanez-Tallon, I., Heintz, N., and Omran, H. (2003). To beat or not to beat: roles of cilia in development and disease. Hum. Mol. Genet. *12*, 27–35.

Ibanez-Tallon, I., Pagenstecher, A., Fliegauf, M., Olbrich, H., Kispert, A., U.-Ketelsen, P., North, A., Heintz, N., and Omran, H. (2004). Dysfunction of axonemal dynein heavy chain Mdnah5 inhibits ependymal flow and reveals a novel mechanism for hydrocephalus formation. Hum. Mol. Genet. *13*, 2133–2141.

Kaiser, P. (1960). Die Leistungen des Flimmerepithels bei der Fortbewegung der Basommatophoran. Z. Wiss. Zool. *162*, 368–393.

Kajava, A. V. (1998). Structural diversity of leucine-rich repeat proteins. J. Mol. Biol. *277*, 519–527.

Kamiya, R. (1988). Mutations at twelve independent loci result in absence of outer dynein arms in *Chlamydomonas reinhardtii*. J. Cell Biol. *107*, 2253–2258.

Kamiya, R., and Okamoto, M. (1985). A mutant of *Chlamydomonas reinhardtii* that lacks the flagellar outer dynein arm but can swim. J. Cell Sci. *74*, 181–191.

King, S. J., and Dutcher, S. K. (1997). Phosphoregulation of an inner dynein arm complex in *Chlamydomonas reinhardtii* is altered in phototactic mutant strains. J. Cell Biol. *136*, 177–191.

King, S. M., and Kamiya, R. (2008). Axonemal dyneins: assembly, structure and force generation. In: The *Chlamydomonas* Sourcebook: Cell Motility and Behavior, Vol. *3*, ed. G. B. Witman, San Diego: Academic Press, 131–208.

King, S. M., and Patel-King, R. S. (1995). The $M_{(r)}$ = 8,000 and 11,000 outer arm dynein light chains from *Chlamydomonas* flagella have cytoplasmic homologues. J. Biol. Chem. *270*, 11445–11452.

Lechtreck, K. F., Delmotte, P., Robinson, M. L., Sanderson, M. J., and Witman, G. B. (2008). Mutations in hydin impair ciliary motility in mice. J. Cell Biol. *180*, 633–643.

Liu, Z., Takazaki, H., Nakazawa, Y., Sakato, M., Yagi, T., Yasunaga, T., King, S. M., and Kamiya, R. (2008). Partially functional outer-arm dynein in a novel *Chlamydomonas* mutant expressing a truncated γ heavy chain. Eukaryot. Cell *7*, 1136–1145.

Loges, N. T., *et al*. (2008). DNAI2 mutations cause primary ciliary dyskinesia with defects in the outer dynein arm. Am. J. Hum. Genet. *83*, 547–558.

Lorenzo, I. M., Liedtke, W., Sanderson, M. J., and Valverde, M. A. (2008). TRPV4 channel participates in receptor-operated calcium entry and ciliary beat frequency regulation in mouse airway epithelial cells. Proc. Natl. Acad. Sci. USA *105*, 12611–12616.

Machemer, H. (1972). Ciliary activity and the origin of metachrony in *Paramecium*: effects of increased viscosity. J. Exp. Biol. *57*, 239–259.

MacRae, E. K. (1967). The fine structure of sensory receptor processes in the auricular epithelium of the planarian, *Dugesia tigrina*. Z. Zellforsch. Mikrosk. Anat. *82*, 479–494.

Marszalek, J. R., Ruiz-Lozano, P., Roberts, E., Chien, K. R., and Goldstein, L.S.B. (1999). Situs inversus and embryonic ciliary morphogenesis defects in mouse mutants lacking the KIF3A subunit of kinesin-II. Proc. Natl. Acad. Sci. USA *96*, 5043–5048.

Martin, G. G. (1978). A new function of rhabdites; mucus production for ciliary gliding. Zoomorphologie *91*, 235–248.

Miller, S. L. (1974). Adaptive design of locomotion and foot form in prosobranch gastropods. J. Exp. Mar. Biol. Ecol. *14*, 99–156.

Mitchell, D. R., and Kang, Y. (1991). Identification of *oda6* as a *Chlamydomonas* dynein mutant by rescue with the wild-type gene. J. Cell Biol. *113*, 835–842.

Mitchell, D. R., and Rosenbaum, J. L. (1985). A motile *Chlamydomonas* flagellar mutant that lacks outer dynein arms. J. Cell Biol. *100*, 1228–1234.

Newmark, P. A., Reddien, P. W., Cebria, F., and Sánchez Alvarado, A. (2003). Ingestion of bacterially expressed double-stranded RNA inhibits gene expression in planarians. Proc. Natl. Acad. Sci. USA *100*, 11861–11865.

Newmark, P. A., and Sánchez Alvarado, A. (2002). Not your father's planarian: a classic model enters the era of functional genomics. Nat. Rev. Genet. *3*, 210–219.

Patel-King, R. S., and King, S. M. (2009). An outer arm dynein light chain acts in a conformational switch for flagellar motility. J. Cell Biol. *186*, 283–295.

Pazour, G. J., Dickert, B. L., Vucica, Y., Seeley, E. S., Rosenbaum, J. L., Witman, G. B., and Cole, D. G. (2000). *Chlamydomonas* IFT88 and its mouse homologue, polycystic kidney disease gene tg737, are required for assembly of cilia and flagella. J. Cell Biol. *151*, 709–718.

Pfister, K. K., Fay, R. B., and Witman, G. B. (1982). Purification and polypeptide composition of dynein ATPases from *Chlamydomonas* flagella. Cell Motil. *2*, 525–547.

Riedel, I. H., Kruse, K., and Howard, J. (2005). A self-organized vortex array of hydrodynamically entrained sperm cells. Science *309*, 300–303.

Rink, J. K., Gurley, K. A., Elliott, S. A., and Sánchez Alvarado, A. (2009). Planarian Hh signaling regulates regeneration polarity and links Hh pathway evolution to cilia. Science *326*, 1406–1410.

Robb, S. M., Ross, E., and Sánchez Alvarado, A. (2008). SmedGD: the *Schmidtea mediterranea* genome database. Nucleic Acids Res. *36*, 599–606.

Rompolas, P., Patel-King, R., and King, S. M. (2009). *Schmidtea mediterranea*: a model system for analysis of motile cilia. Methods Cell Biol. *93*, 81–98.

Rutland, J., Cox, T., Dewar, A., Rehahn, M., and Cole, P. (1983). Relationship between dynein arms and ciliary motility in Kartagener's syndrome. Eur. J. Respir. Dis. Suppl. *128*, 470–472.

Shah, A. S., Ben-Shahar, Y., Moninger, T. O., Kline, J. N., and Welsh, M. J. (2009). Motile cilia of human airway epithelia are chemosensory. Science *325*, 1131–1134.

Sleigh, M. A. (1974). Metachronism of cilia of metazoa. In: Cilia and Flagella, ed. M. A. Sleigh, London: Academic Press, 287–304.

Smith, D. J., Gaffney, E. A., and Blake, J. R. (2008). Modeling mucociliary clearance. Respir. Physiol. Neurobiol. *163*, 178–188.

Sorin, M. M. (2007). Metachronal wave formation in a model of pulmonary cilia. Comput. Struct. *85*, 763–774.

Teff, Z., Priel, Z., and Gheber, L. A. (2008). The forces applied by cilia depend linearly on their frequency due to constant geometry of the effective stroke. Biophys. J. *94*, 298–305.

Timmons, L., Court, D. L., and Fire, A. (2001). Ingestion of bacterially expressed dsRNAs can produce specific and potent genetic interference in *Caenorhabditis elegans*. Gene *263*, 103–112.

Timmons, L., and Fire, A. (1998). Specific interference by ingested dsRNA. Nature *395*, 854

Wakabayashi, K., and King, S. M. (2006). Modulation of *Chlamydomonas reinhardtii* flagellar motility by redox poise. J. Cell Biol. *173*, 743–754.

Wood, C. R., Hard, R., and Hennessey, T. M. (2007). Targeted gene disruption of dynein heavy chain 7 of *Tetrahymena thermophila* results in altered ciliary waveform and reduced swim speed. J. Cell Sci. *120*, 3075–3085.

Wu, H., Maciejewski, M. W., Marintchev, A., Benashski, S. E., Mullen, G. P., and King, S. M. (2000). Solution structure of a dynein motor domain associated light chain. Nat. Struct. Biol. *7*, 575–579.

Zayas, R. M., Hernandez, A., Habermann, B., Wang, Y., Stary, J. M., and Newmark, P. A. (2005). The planarian *Schmidtea mediterranea* as a model for epigenetic germ cell specification: analysis of ESTs from the hermaphroditic strain. Proc. Natl. Acad. Sci. USA *102*, 18491–18496.